Proceedings of Iran International Aluminum Conference (IIAC2014)
May 25-26, 2014, Tehran, I.R. Iran

Adsorption of Fluoride Gases in Aluminum Production using Nano Technology

Kambiz Bordbari [*1], Mohsen Ameri Siahooei[2], Ahmad Irannejad[3], Gholam Reza Khayati[4]

[1,3,4]Materials Science and Engineering Department, Shahid Bahonar University of Kerman, P.O. Box: 76135-133, Kerman, Iran

[2]Almahdi-Hormozal Aluminium Smelter, Bandar abass, P.O. Box: 79171-7-6385, Iran

Abstract: HF,Cf_4,C_2F_6 and SiF4 are the main gaseous fluorides evolved in the Hall-Heroult process. However, the major contributor of fluoride is HF. Since these gases are very toxic, they must be adsorbed from environment. In this research, adsorption of HF,Cf_4,C_2F_6 and SiF_4 in aluminium smelter is discussed and compared. Due to the capability of nanotubes in gas adsorption, this study has been conducted to figure out the adsorption of fluoride gases on (8,8) armchair carbon nanotubes (CNTs). Lennard-Jones potential was used for gas-gas and gas-carbon nanotube interactions. In addition, the potential parameters for the carbon-gas and carbon-carbon interactions were obtained from the Lorenz-Berthelot combining rules. The simulation results showed that this adsorption can be a possible solution for separation of toxic gases from environment. The proposed method provides a new horizon in the aluminium industry.

Keywords: "carbon nanotube, monte carlo simulation, adsorption gas;"

Introduction

Perfluorcarbon(PFC,e.g. tetrafluoromethane and hexafluoroethane) emissions are harmful to the environment because of their global warming potential and, therefore, it is a challenge for the aluminum industry to reduce the evolution of such gases.Tetrafluoromethane,CF_4,and hexafluoroethane, C_2F_6, are greenhouse gases emitted when anode effects occur during primary aluminium production (1) . Accurate accounting and inventory of PFC emissions is increasingly important as primary aluminum producers have made commitments, either made voluntarily or based on national regulatory requirements, to meet GHG emissions objectives. tetrafluoromethane (CF_4) and hexafluoroethane (C_2F_6), are emitted from aluminum smelters during anode effects (AEs). An anode effect occurs when the current density in the anode exceeds the critical current density. The critical current density depends on temperature and chemical composition of the electrolytic bath. Decreasing alumina content in the electrolytic bath is the most important factor and when it gets too low (below 2%), the cell voltage rises and bath and carbon anodes begin to react. Aluminum smelters are considered to be the largest anthropogenic source of PFC emissions worldwide.

In 1991, Iijima announced the discovery of multiwalled carbon nanotubes as a byproduct in fullerene production [1-2].

Since then, great efforts were made to improve the yield during the preparation and purification. Single-walled carbon nanotubes (SWNT) are available since 1992 in enough quantities to be studied, and immediately attracted attention because of potential technological applications and also from basic research perspective because it was the first from of carbon that could provide physical realizations of ideal systems.

Single-walled carbon nanotubes could be considered as the result of bisecting a C_{60} molecule at the equator and the two resulting hemispheres are joined with a cylindrical tube one monolayer thick and with the same diameter as C_{60}. If the C_{60} molecule is bisected normal to a 5-fold axis, an armchair tubule is obtained, whereas if the bisection is made normal to a 3-axis, a zigzag type tubule is obtained. Other chiral tubles can be formed with a screw axis along the axis of the tuble. Carbon nanotubes can be specified in terms of the tuble diameter d_t,and chiral angle θ, that define the chiral vector. $c_h = na_1 + ma_2$ .The tube can then be identified using pair of integers (n,m) that define the chiral vector [3].

Carbon nanotubes have been found to assemble in bundles where the tubes are in a hexagonal array with different lengths. Carbon nanotubes have gathered much attention both from fundamental science and technological interests. Very high chemical stability and mechanical strength made the carbon nanotube a very important material in nanotechnology. Existing theoretical literature suggests that defect-free, pristine carbon nanotubes (CNTs) interact weakly with many gas molecules like $H_2O, CO, NH_3, H_2,$ and so on[4].

In this work, grand canonical Monte Carlo (GCMC) method is used to study the Fluoride compounds adsorption gas on carbon nanotube. Single-Walled carbon nanotubes are selected to be the adsorbent. To make a comprehensive work, the influence of temperature as well as pressures on the adsorption is also studied.

The simulation results in this work can be used to optimize the Fluoride compounds adsorption at a given pressures and temperatures.

Simulation Method

The Monte carlo statistical mechanical simulation were carried out in standard manner using the Metropolis sampling technique in canonical (T,V,N) ensamble. In this work, all of the particles include Sulfur compounds molecules, and carbon atoms are treated as structureless spheres. Particle-Particle interactions between them are modeled with Lennard-Jones potential located at the mass-center of the particles.In this work, as in the works of many researchers, the cut and shifted Lennard-Jone (LJ) potential was used to represent the interaction between Sulfur compounds molecules.

$$\phi_{ff}(r)=\begin{bmatrix}\phi_{ij}(r)-\phi_{ij}(r_c) & r<r_c\\ 0 & r\geq r_c\end{bmatrix} \qquad (1)$$

Where r is the interparticle distance, r_c is the cut off radius, $r_c=5\sigma_{ff}$. ϕ_{ij} is the full LJ potential, $\phi_{ij}=4\varepsilon_{ff}\left[\left(\sigma_{ff}/r\right)^{12}-\left(\sigma_{ff}/r\right)^{6}\right]$, where ε_{ff} and δ_{ff} are the energy and size parameters of the fluid .They are 460 and 2.75nm for Hf also 220 and 5.3nm for C_2f_6 also 134 and 4.662 for Cf_4 also 171.9 and 4.88nm for SiF4 here [5-6-7] respectively. The interaction between the wall and a hydrogen sulfide molecule is calculated by the site-to-site method [8-9].

$$U_{fw}=4\varepsilon_{fw}\sum_{i=1}^{N_f}\sum_{j=1}^{Ncabon}\left[\left(\frac{\sigma_{fw}}{r_{ij}}\right)^{12}-\left(\frac{\sigma_{fw}}{r_{ij}}\right)^{6}\right] \qquad (2)$$

For exampe Where N_f is the number of sulfur dioxide gas molecules, N_{carbon} is the number of carbon atoms of the wall of SWNT. ε_{fw} and δ_{fw} are the cross-energy and size parameters, which are obtained from the Lorentz-Berthelot (LB) combining rules. Energy and size parameters of carbon atoms are 28.0 and 0.34nm, respectively[10].

r_{ij} is the distance between a gas hydrogen sulfide molecule and an atom of the wall of SWNT.

Lorentz-Berthelot rules are used to calculate the parameters of interaction between different kinds of particles. In this calculation, all of the particles are regarded as spheres. Interaction among particles are modeled with Lennard-Jones potential acted on the mass center.The initial configuration was generated randomly (Figure1). For a fixed cell, three types of moves were used to generate a markov chain, including moving, creating, and deleting a molecule and make new configurations. The three types of moves have the same probability and each has different receiving opportunities.Configurations are accepted when they obey Metropolis's Sampling scheme in proportion to $\exp\left(\frac{-\Delta E}{KT}\right)$ where ΔE is the change of total energy in the system.

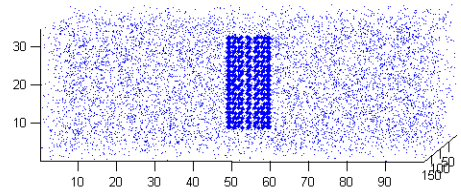

Figure1 initial configuration

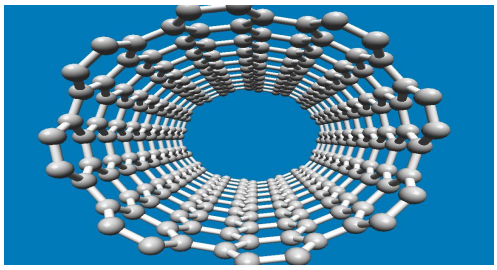

Figure 2 Armchiar (8,8)

To insure good thermodynamical averages, for a single isotherm point typically 5×10^6 moves have been performed to equilibrate the system. for each of five hundred configuration, one configuration is selected, and names snapshot. diagram energy of produced configuration to namber of snapshot show that system reach to the equilibrium.

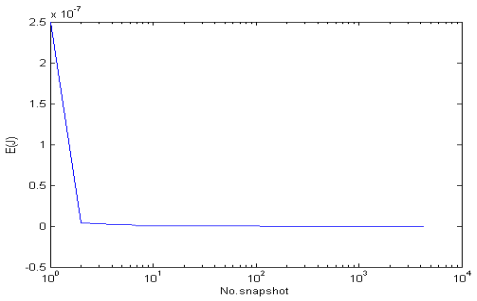

Figure 3 snapshot to percent of abundance

The ensemble average energy of system for second helf of snap shots is drawn, and initial part is discarded. Because initial part far away to the equilibrium. diagram

of energy for second helf, show that, the system reach to equilibrium.

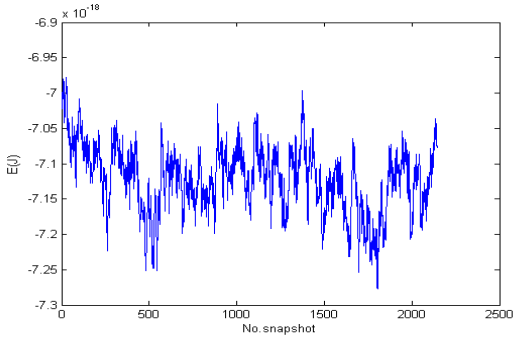

Figure 4 snapshot for second helf to percent of abundance

The statistical error have been reported in this work.STDEW is the standard deviation of the calculated average in the simulation of eight number is 0.64% (simulatin error).The dimensions of simulation cell is $(200\times100\times34.5)A^{\circ}$. We considered single-walled armchair (8,8) nanotubes with open edge (Figure2). The number of carbon atom is 320. The diameters of the nanotubes is $10.854A^{\circ}$, and the averge bond length is $24A^{\circ}$ respectively. The number of molecules gas calculated by virial equation of state and input to the GCMC calculation. The equation of state of real gases is best represented, by the series (equation 3)

$$PV_m = RT\left[1+\frac{B_{(T)}}{V_m}+\frac{C_{(T)}}{V_m^2}+\frac{D_{(T)}}{V_m^3}+\cdots\cdots\cdots\right] \quad (3)$$

Where $B_{(T)}, C_{(T)}$, and $D_{(T)}$ are respectively termed the second, third, and fourth virial coefficients.(P) is the pressure, (V_m) is molar volume, (T) the absolute temperature, and (R) the gas constant [11].

Results and Discussions

Comparative investigation of adsorption rate of CF_4, C_2F_6, HF, SiF4 gases at the same pressure and different temperatures in carbon nanotubes using Monte Carlo simulation

In this study, the effect of temperature on adsorption of gaseous fluoride compounds of aluminum electrolysis process in single-walled carbon nanotubes is investigated. The first gas is C_2F_6 and used temperatures are: 180, 323 and 195.1 K and constant pressure is equal to 11 MPa.
Figure 5 indicates the density distribution of C_2F_6 gas in terms of distance from the axis of nanotube at different temperatures. The number of gas molecules In these situation is calculated by Second virial coefficient [12]. And the potential parameters of lonard jones are extracted [13].

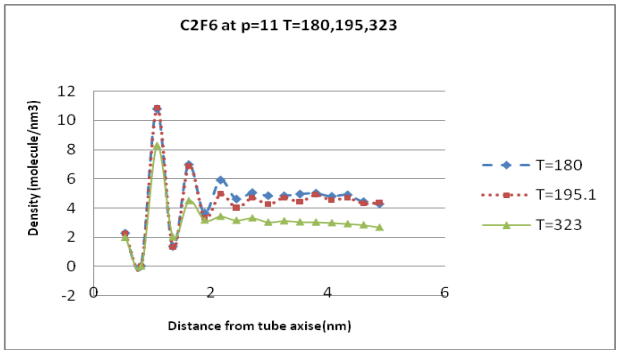

Figure 5 distribution of C_2F_6 adsorption density versus the distance from the axis of nanotube at different temperatures and pressure of 11 Mpa.

As it can be seen from Figure 5, increasing of temperature decreases the density of adsorption on carbon nanotubes. At temperature of 180 K, maximum distribution of C_2f_6 gas is around the nanotube wall. In this case the maximum temperature and maximum absorption peak of density are calculated. The density decreases with distance from the axis of the nanotube.
Table 1 shows the number of gas molecules presented in simulation cells, which is calculated by the second Virial coefficient using the specified temperature. According to Table 1 it is clear that total density of C_2F_6 gas is reduced by increasing temperature. In Figure 6 the changes of C_2f_6 density is plotted versus temperature. The negative slope of the graph in this figure represents the C_2F_6 density decreases with increasing temperature.

Table 1 The inside, outside and total density of C_2F_6 adsorption in single-walled carbon nanotube at different temperatures.

Temperature (k)	180	195.1	323
Second virial coefficient $(cm^3/mole)$	-815	-611	-199
Number of molecules	3053	2819	1701
Inside density $molecules/nm^3$	2.25	2.24	1.96
Outside density $molecules/nm^3$	4.99	4.68	3.62
Total density $molecules/nm^3$	4.82	4.53	3.52

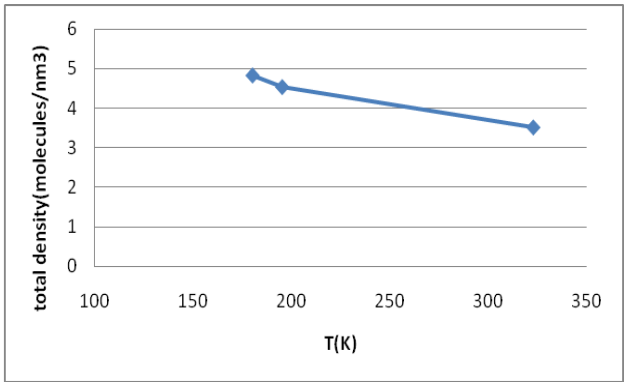

Figure 6 The effect of temperature on C_2F_6 gas adsorption.

Figure 7 shows adsorption density of Cf_4 gas versus the distance from the axis of nanotube at different temperatures. The number of gas molecules is calculated by Second virial coefficient [14]. And the potential parameters of lonard jones have been taken [10]. The applied temperatures are: 225, 323, and 800 K and pressure is constant and equal to 11 MPa.

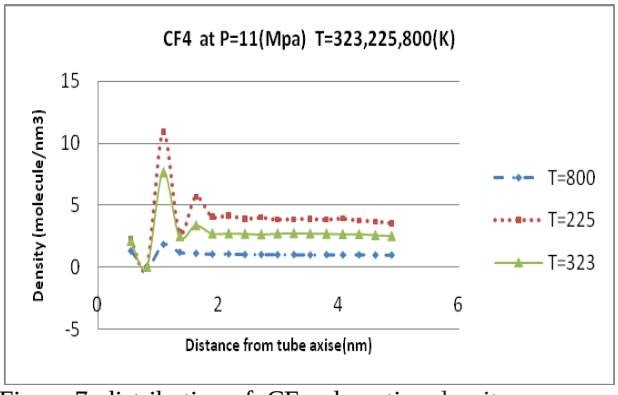

Figure 7 distribution of CF_4 adsorption density versus the distance from the axis of nanotube at different temperatures and pressure of 11 Mpa.

As it can be seen from Figure 7, with increasing of temperature the adsorption density on carbon nanotube is reduced and Most of the CF_4 gas distribution is around the nanotube wall at 225 K.

Table 2 The inside, outside and total density of CF_4 adsorption in single-walled carbon nanotube at different temperatures

Temperature (k)	225	323	800
Second virial coefficient $(cm^3/mole)$	-815	-611	-199
Number of molecules	3053	2819	1701
Inside density $molecules/nm^3$	2.31	2.12	1.29
Outside density $molecules/nm^3$	4.65	3.16	1.08
Total density $molecules/nm^3$	4.51	3.09	1.09

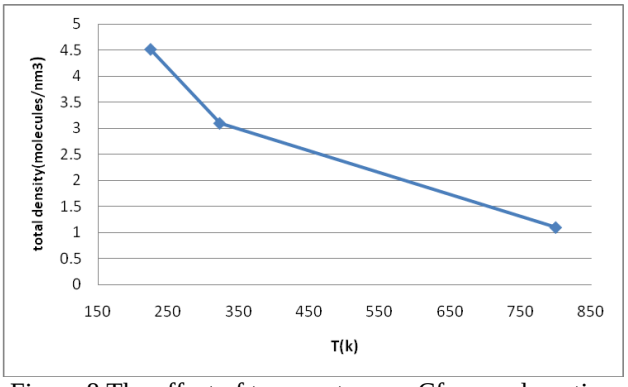

Figure 8 The effect of temperature on Cf_4 gas adsorption

Table 2 indicates the number of CF_4 gas molecules calculated in specifies temperature. From this table and Figure 8 descending process of gas adsorption on carbon nanotube is observed with increasing temperature.

The third gas under investigation is HF. Figure 9 shows adsorbtion density of HF versus the distance from the axis of the nanotube at different temperatures. The number of gas molecules is calculated by Second virial coefficient [5]. And the potential parameters of lonard jones have been taken [10]. Temperatures used are: 275, 320, 440 K, and constant pressure is equal to 7 MPa intended.
As it is clear from figure 9, increasing the temperature decreases the density of adsorption on carbon nanotubes. At 227 K, the maximum amount of HF distribution is along the axis of nanotubes which is Similar to the CF_4 and C_2F_6 gases.

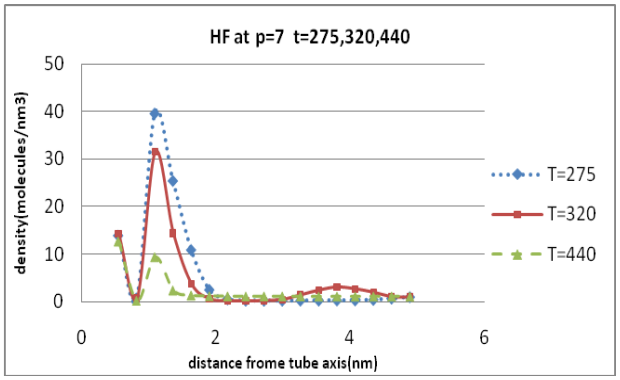

Figure 9 distribution of HF adsorption density versus the distance from the axis of nanotube at different temperatures and pressure of 7 Mpa.

Similar to C_2F_6 and CF_4 gases, the amount of HF gas adsorption decreases with increasing temperature. This found can be seen in Table 3 and Figure 10.

Table 3 The inside, outside and total density of HF adsorption in single-walled carbon nanotube at different temperatures

Temperature (k)	275	320	440
Second virial coefficient $(cm^3/mole)$	39.6	12.15	2.07
Number of molecules	1272	1093	795
Inside density $molecules/nm^3$	13.97	4.19	12.69
Outside density $molecules/nm^3$	11.22	6.72	2.23
Total density $molecules/nm^3$	11.39	7.18	2.89

Table 4 The inside, outside and total density of SiF4 adsorption in single-walled carbon nanotube at different temperatures

Temperature (k)	293	323	450
Coefficient Second virial $(cm^3/mole)$	-145.6	-109.4	-34.5
Number of molecules	1193	1082	777
Inside density $molecules/nm^3$	2.19	2.22	2.49
Outsidedensity $molecules/nm^3$	2.94	2.59	1.40
Total density $molecules/nm^3$	2.89	2.56	1.47

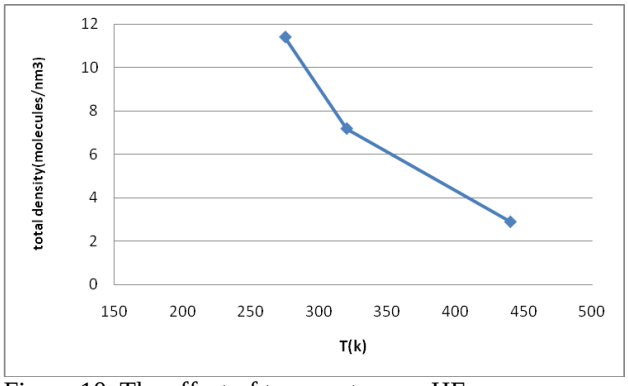

Figure 10 The effect of temperature on HF gas adsorption

We continued our study with SiF4 gas. In Figure 11 adsorbtion density of SiF4 versus the distance from the axis of the nanotube is investigated at different temperatures. The number of gas molecules is calculated by Second virial coefficient [15]. And the potential parameters of lonard jones have been considered [10].
Applied temperatures are: 293, 323 and 450 K and pressure is constant and equal to 7 MPa.

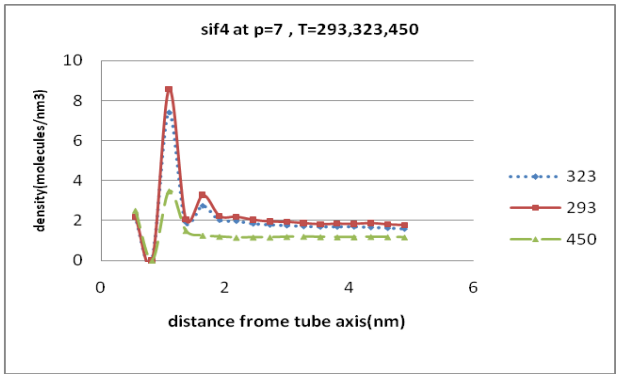

Figure 11 distribution of SiF4 adsorption density versus the distance from the axis of nanotube at different temperatures and pressure of 7 Mpa

As it can be seen from this figure, increasing the temperature decreases the density of adsorption on carbon nanotubes and the maximum SiF4 distribution along the axis of nanotubes is at 293 K. Despite we applied same pressure and close temperatures for both SiF4 and HF gases, but the inside, outside and total density of SiF4 are much lower than those of HF. pressure and temperature are relatively similar to those HF . This fact is clear by comparing the Tables 3 and 4 and Figures 10 and 12.

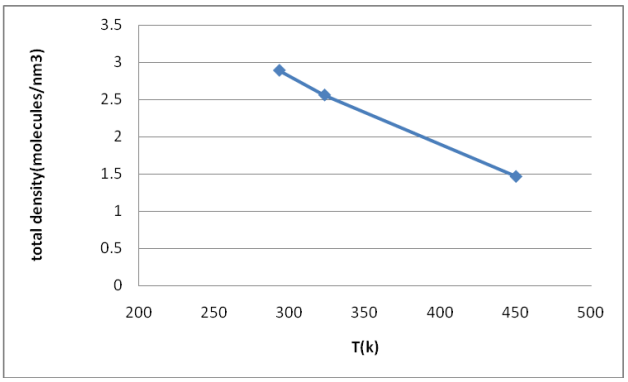

Figure 12 The effect of temperature on SiF4 gas adsorption

Comparative investigation of adsorption rate of Cf_4, C_2F_6, Hf and SiF4 at the same temperature and different pressures on carbon nanotubes using Monte Carlo simulation

In this section the effect of pressure on the fluoride compounds adsorption in single-walled carbon nanotubes (arm chair(8,8)) in aluminum industry has been studied. We investigated on four gases: C_2F_6, Cf_4, Hf ,and SiF4 at pressures: 3,13,7, and 11 MPa, and at constant temperature of 323 K.
Figure 13 shows the distribution of C_2F_6 gas in terms of the distance from nanotube axis. The number of gas molecules is calculated with respect to the second factor Viiryal [12]. And Potential parameters are calculated [5].

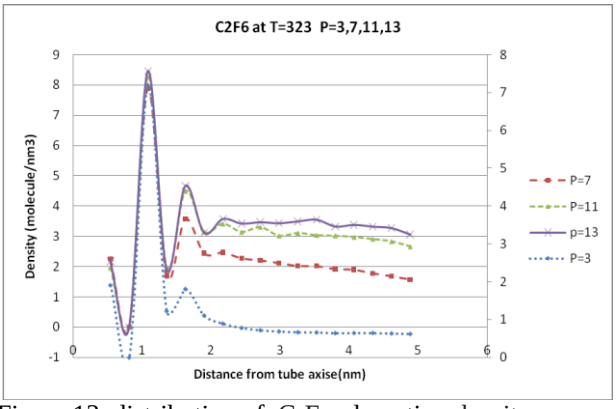

Figure 13 distribution of C_2F_6 adsorption density versus the distance from the axis of nanotube at different pressures and temperature of 323 K

From this figure it can be seen that the maximum adsorption near the axis of nanotube has been occurred with very close values, but the overall density calculated at a pressure of 13 MPa is almost doubled compared to the pressure of 3 Mpa which is due to the absorption changes in areas away from the nanotube surface.
Diagrams in Figures 14, 15 and 16, respectively, related to gases Cf_4, HF and SiF4. the results indicate the maximum adsorption of the gases Occurs in maximum pressure.

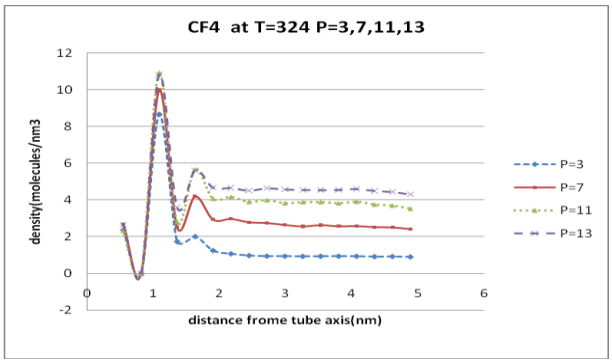

Figure 1 distribution of CF_4 adsorption density versus the distance from the axis of nanotube at different pressures and temperature of 323 K

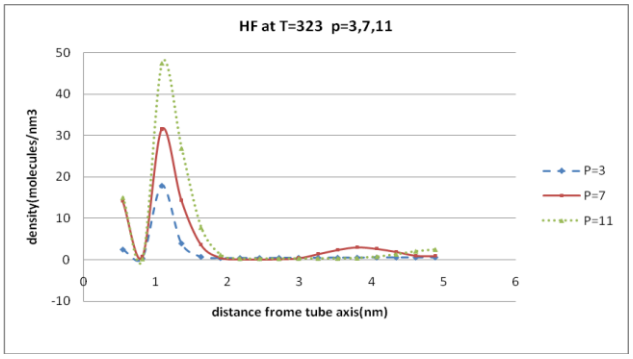

Figure 25 distribution of HF adsorption density versus the distance from the axis of nanotube at different pressures and temperature of 323 K

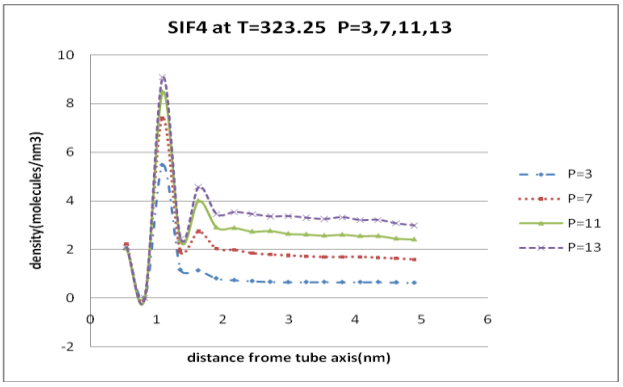

Figure 16 distribution of SiF4 adsorption density versus the distance from the axis of nanotube at different pressures and temperature of 323 K.

From above figures, it can be found that in addition to the first maximum adsorption peak at the closest point on the surface of the nanotube there is a weak adsorption peak at a short distance away from the first one which is caused by the second regular layer of accumulated molecules.
Another notable point is related to HF gas. This gas is very sensitive to increasing pressure for maximum adsorption in the closest point on the surface of nanotube.
Supplemented information in Tables 5 to 8 represent the adsorption density of CF_4, C_2F_6, HF and SiF4 gases at different pressures. According to these tables and figures 17 to 20, with increasing gas pressure, the fluoride adsorption on carbon nanotubes increases and there is a direct relationship between pressure and adsorption density.

Table 5 The inside, outside and total density of HF adsorption in single-walled carbon nanotube at 323 k and different pressures

Pressures	3	7	11	13
Second virial coefficient $(cm^3/mole)$	-109.4	-109.4	-109.4	-109.4
Number of molecules	666	1082	1701	2015
Inside density $molecules/nm^3$	2.04	2.22	2.04	2.09
Outside density $molecules/nm^3$	1.38	2.59	2.43	3.89
Total density $molecules/nm^3$	1.42	2.56	2.35	3.78

Table 6 The inside, outside and total density of SiF4 adsorption in single-walled carbon nanotube at 323 k and different pressures

Pressures	3	7	11	13
Second virial coefficient $(cm^3/mole)$	12.5	12.5	12.5	12.5
Number of molecules	468	795	1717	2030
Inside density $molecules/nm^3$	2.43	6.19	4.99	7.63
Outside density $molecules/nm^3$	3.00	5.72	5.35	8.20
Total density $molecules/nm^3$	2.97	5.15	5.15	8.1

Table 7 The inside, outside and total density of CF_4 adsorption in single-walled carbon nanotube at 323 k and different pressures

Pressures	3	7	11	13
Second virial coefficient $(cm^3/mole)$	-72.4	-72.4	-72.4	-72.4
Number of molecules	666	1082	1701	2015
Inside density $molecules/nm^3$	2.36	2.67	2.31	2.63
Outside density $molecules/nm^3$	2.18	3.68	4.65	5.00
Total density $molecules/nm^3$	2.19	3.62	4.51	4.85

Table 8 The inside, outside and total density of C_2F_6 adsorption in single-walled carbon nanotube at 323 k and different pressures

Pressures	3	7	11	13
Second virial coefficient $(cm^3/mole)$	-199	-199	-199	-199
Number of molecules	464	1082	1701	2010
Inside density $molecules/nm^3$	1/91	2.24	1.96	2.16
Outside density $molecules/nm^3$	1.82	2.97	3.62	3.69
Total density $molecules/nm^3$	1.83	2.92	3.52	3.6

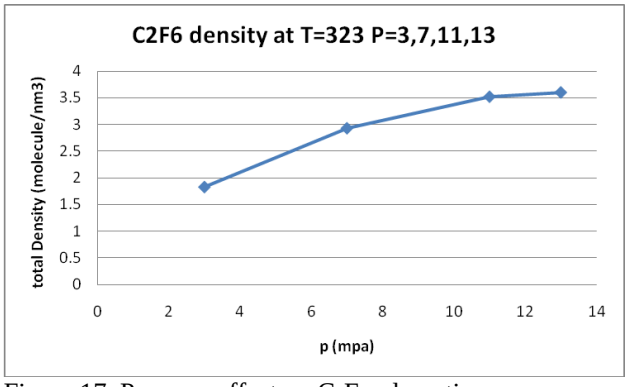

Figure 17 Pressure effect on C_2F_6 adsorption

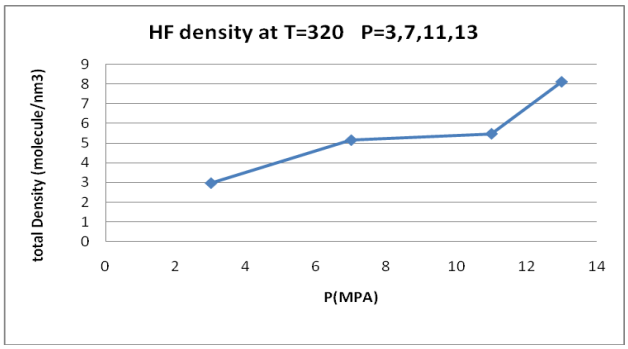

Figure 18 Pressure effect on Hf adsorption

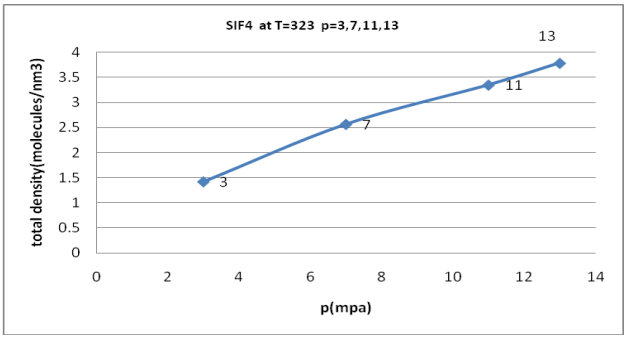

Figure 19 Pressure effect on SiF4 adsorption

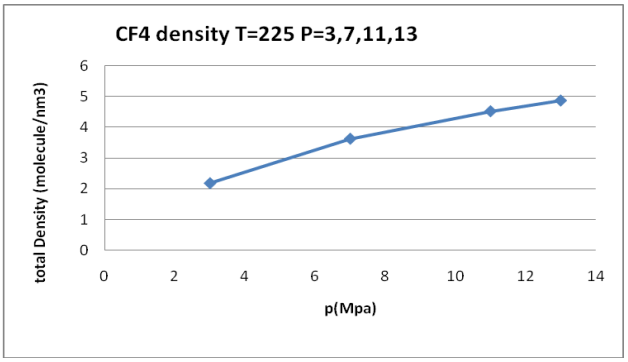

Figure 20 Pressure effect on CF_4 adsorption

Comparative study of adsorption of C_2F_6, HF, SiF4 and CF_4 gases in tmperature of 323 k and pressure of 7 Mpa On carbon nanotubes using Monte Carlo simulation

In this section, we applied Monte Carlo simulation for original system. The calculated number of molecules is 1082 in the gas simulation cell. number of gas molecules is calculated with respect to the second factor of Viriyal [5-12-14-15]. Potential of the parameters are extracted [10].

Figure 21 shows the density distribution of these gases versus the distance from axis of the nanotube.

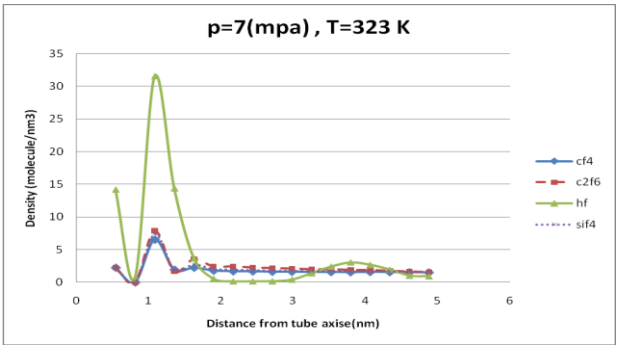

Figure 21 Adsorption of fluoride gases at a pressure of 7 Mp and temperature of 323 K

Figure 21 indicates that there is a big difference between the Hf adsorption and other gases at the same temperature and pressure which represents that this gas is absorbed six

times more than other gases at the closest point on the inside surface of the nanotube.

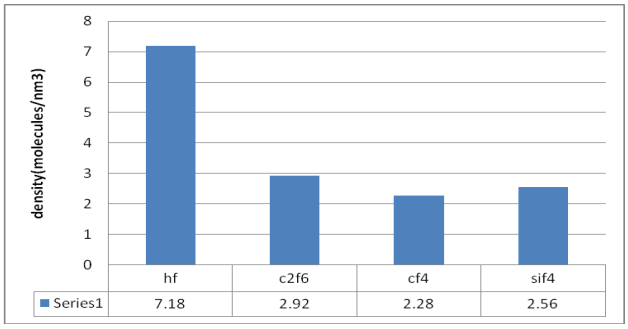

Figure 22 comparison of adsorption density of fluoride gases at pressure of 7 mp and temperature of 323 K.

Figure 22 shows a comparison of the adsorption density of four gases. From this figure it is clear that HF absorption rate is twice of other gases.

Conclusion

The effect of temperature and pressure on fluoride gases indicate that gas absorption in single-wall armchair (8,8) nanotubes will increase with decreasing temperature.

Moreover, with increasing pressure, the gas absorption rate will be added.

It was observed that C_2f_6 is less sensitive to temperature changes while HF is more sensitive to changes of pressure in compare with other Fluoride compounds.

Ultimately, at the same temperature and pressure, HF has the maximum rate of adsorption. In future work, we are going to obtain the practical results of the proposed method.

References

[1] Dae-Hwang Yoo, Gi-Hong Rue,. 2001,.study of Nitrogen Adsoded on Single-walled Carbon Nanotube Bundles, J. phys Chem. B 2002, 106, 3371-3374

[2] H. Nguyen, V. Mai,. Effect of NH_3 gas on the electrical properties of single-walled carbon nanotube bundles, Sensors and Actuators B 113 (2006) 341-346

[3] P. Juan, S. Fabian,.2003, N_2 Physisorption on Carbon Nanotubes: Computer Simulation and Experimental Results,J. phys. Chem. B 2003, 107, 8905-8916

[4] Andzelm. J, Govind. Niranjan,.2006, Nanotube-based gas sensors-Role of structural defects, Chemical physics Letters 421 (2006) 58-62

[5].S. MURAD,K.A.MANSOUR "A model inter molecular potential for hydrogen fluoride including polarizability" CPIEMICAL PHYSICS LETTERS- 131, number I,2-(1986)

[6].L. Meng , Y. Duan "Site–site potential function and second virial coefficients for linear molecules" Molecular Physics - 104, Issue 18, (2006).

[7].CHJ.Johnson,TH.Spurling" Mixture virial coefficients for the Hamann-Lambert model for globular molecules" *Australian Journal of Chemistry* 24(12) 2449 – 2459.

[8] Chong Gu,Guang-Hua Gao,Yang-Xin Yu,Zong-Qinga Mao, International Journal of Hydrogen Energy , 2001, 26, 691-696.

[9] Vahan V. Simonyan, J.Karl Johnson, Journal of Alloys and Compound, 2002, 330-332, 659-665.

[10] Skelland, A. H. P., 1985, Diffusional mass transfer, New York: Wiley, pp 482.

[11] J. H. Dymond and E. B. Smith., 1980, the Virial coefficients of pure Gases and Mixtures, A Critical Compilation, Introduction.

[12] (E.M. Dantzler and C.M. Knobler, J . Chem., Ithaca 73 1335 (1969).

[13] H. P., 1985, Diffusional mass transfer, New York: Wiley, pp 482.

[14] K.E.MacCormack and W.G. Schneider, J. chem.. Phys. 19 845,849 (1951) .

[15] (S.D. Hamann,w.j. McManamey, and J.F. Pearse, Trans. Faraday Soc. 49 351(1953) .